# Supporting Information: A Transferable, Multi-Resolution Coarse-Grained Model for Amorphous Silica Nanoparticles

*Andrew Z. Summers*†,‡, *Christopher R. Iacovella*†,‡, *Olivia M. Cane*†,‡, *Peter T. Cummings*†,‡, *Clare McCabe**,†,‡,§

†Department of Chemical and Biomolecular Engineering, ‡Multiscale Modeling and Simulation (MuMS) Center, and §Department of Chemistry, Vanderbilt University, Nashville, Tennessee 37235, United States

Contents of the supporting information are as follows:

- Additional details on the coarse-grained nanoparticle model
  - Golden section spiral algorithm
  - Maximum packing model, $\varphi_b(d, \sigma_b)$
  - Fixed $\varphi_b$ model
- Additional details on the collection of atomistic target data
  - Bulk silica equilibration procedure
  - Carving of nanoparticles from bulk silica
  - Choice of atomistic force field
  - Procedure for collection of target data for nanoparticle-nanoparticle interaction energy
  - Procedure for collection of target data for nanoparticle-alkane cross-interactions
- Equations used from the work of Lee and Hua for CG model comparison
- Excluded states in parameterization of nanoparticle-nanoparticle core interactions
- Interactions between nanoparticles with different $d$, $\sigma_b$, and $\varphi_b$

*Corresponding Author: Clare McCabe, Email: c.mccabe@vanderbilt.edu

## Coarse-grained nanoparticle model (additional details)

### Golden section spiral algorithm

The golden section spiral algorithm used to distribute pseudo-atoms into a spherical shell is included within the mBuild Python package.[1,2] The algorithm itself was adapted from a thread on the numpy-discussion list.[3]

The following equations are used for the golden section spiral algorithm.

$$\varphi = \frac{1}{2}(1 + \sqrt{5})$$

$$l_{\text{incr}} = 2\pi/\varphi$$

$$d_z = 2/n, \text{where } n = \text{the number of pseudo} - \text{atoms}$$

$$\text{bands} = 0, 1, \ldots, n-1, n$$

$$z = \text{bands} \cdot d_z - 1 + \left(d_z/2\right)$$

$$r = \sqrt{1 - z^2}$$

$$a_z = \text{bands} \cdot l_{\text{incr}}$$

$$x = r \cdot \cos a_z$$

$$y = r \cdot \sin a_z$$

Where *x*, *y*, and *z* define lists of the x, y, and z coordinates for all particles around a unit sphere. Particle positions are then scaled by $\frac{1}{2}[d - (\sigma_{\text{b}} + \sigma_{\text{silica}})]$, where *d* is the diameter of the atomistic nanoparticle and $\sigma_{\text{silica}}$ = 0.40323nm is the arithmetic average of $\sigma_{\text{Si}}$ and $\sigma_{\text{O}}$. This ensures the nanoparticle radius remains nominally independent of bead size.

Nanoparticles can be constructed following this algorithm, or by using instantiating the `CG_nano` class, within the NanoOpt Python Package.[4]

**Maximum packing model, $\varphi_b(d, \sigma_b)$**

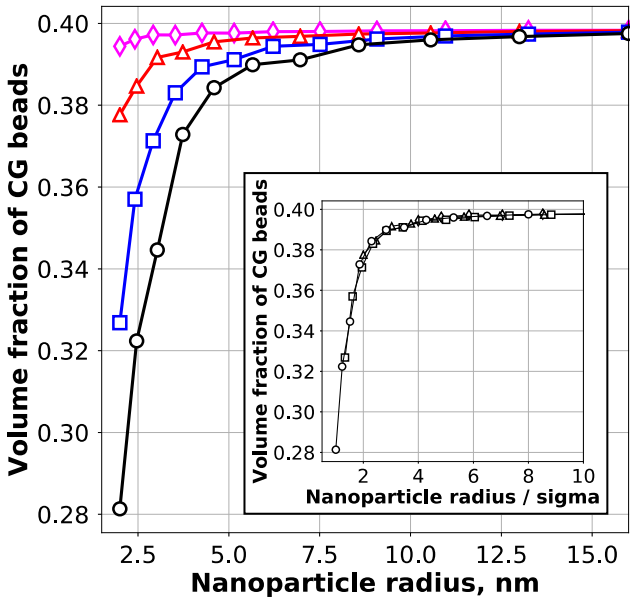


**Figure S1** – Using a maximum packing model, volume fraction of coarse-grained beads within the spherical nanoparticle shell as a function of nanoparticle radius for $\sigma_b$ values of 0.5 (magenta), 1.0 (red), 1.5 (blue), and 2.0nm (black). The inset shows the same data with the nanoparticle radius normalized by $\sigma_b$, where the four curves collapse onto a single line.

Preliminary nanoparticle models featured a maximum packing algorithm, where $\varphi_b$ was maximized without allowing overlap between neighboring beads. Fig. S1 shows that $\varphi_b$ for nanoparticles constructed in this manner is dependent both on the nanoparticle diameter, $d$, and the pseudo-atom diameter, $\sigma_b$. However, the inset of Fig. S1 reveals that $\varphi_b$ is equivalent for values of $d/\sigma_b$. As $d/\sigma_b$ increases, $\varphi_b$ increases, reaching an asymptotic value of roughly 0.4. This phenomenon has profound effects on the transferability of interaction parameters derived for nanoparticles designed using the maximum packing model. Parameters are likely to be transferable between nanoparticles featuring equivalent (or nearly equivalent) values for $\varphi_b$. Thus, parameters would likely be transferable only for nanoparticles with $d/\sigma_b$ values above

*Corresponding Author: Clare McCabe, Email: c.mccabe@vanderbilt.edu 

about 5. Furthermore, if nanoparticles with lower values of $d/\sigma_b$ are included during the optimization, the resulting parameter set will likely have reduced accuracy.

## Atomistic target data

### Bulk silica equilibration

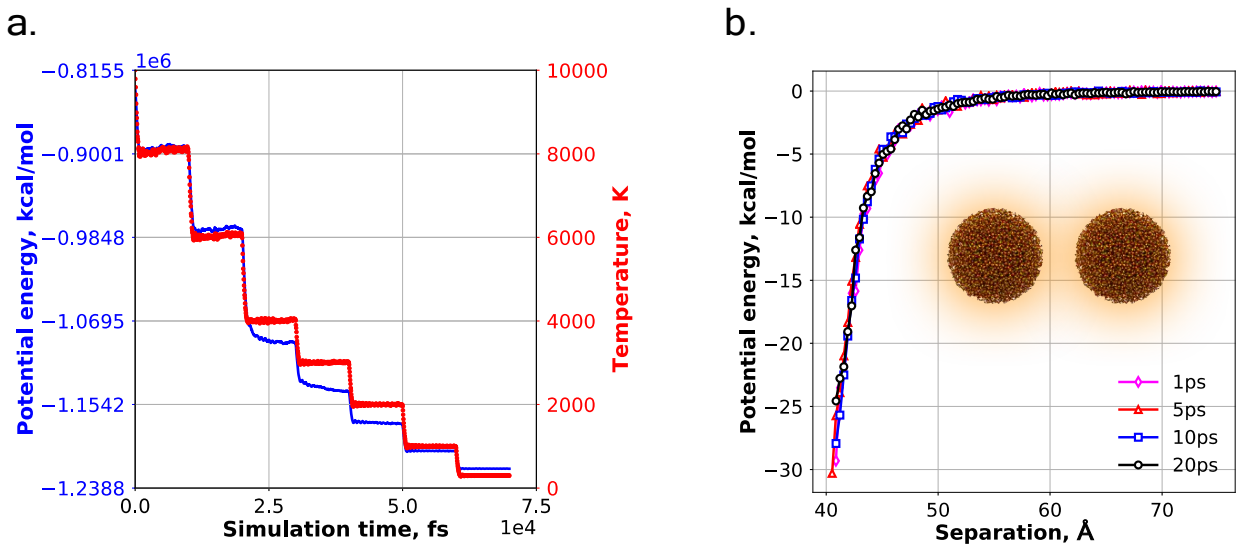


**Figure S2** – a. Total potential energy (blue) and system temperature (red) during the stepwise annealing of the amorphous silica bulk with 10ps spent at each temperature stage. b. Interaction energy between two nanoparticles ($d$=4nm) carved from bulk silica annealed using times of 1, 5, 10, and 20ps spent at each temperature stage.

As described in the main text, the amorphous silica bulk from which atomistic nanoparticles were carved was generated through the procedure described by Litton and Garofalini,[5] where a stoichiometric mixture of Si and O is heated to 10,000K and quenched to 300K through a series of intermediate temperatures, using the ReaxFF force field. The temperature profile of the system through the quenching procedure is shown in Fig. S2a, alongside the potential energy of the system (which is shown to equilibrate quickly at each stage). At each stage the system is held at this temperature for 10ps before advancing to the next stage (directly following the procedure of Litton and Garofalini). We have examined the influence of the time spent at each stage by equilibrating the silica bulk where this time is set to 1, 5, 10, and 20ps and examining the

interaction potential between two nanoparticles carved from each bulk. As shown in Fig. S2b, the quench rate appears to have negligible influence on the interaction potential over the range studied here, providing further confidence that the chosen 10ps is appropriate.

**Nanoparticle carving**

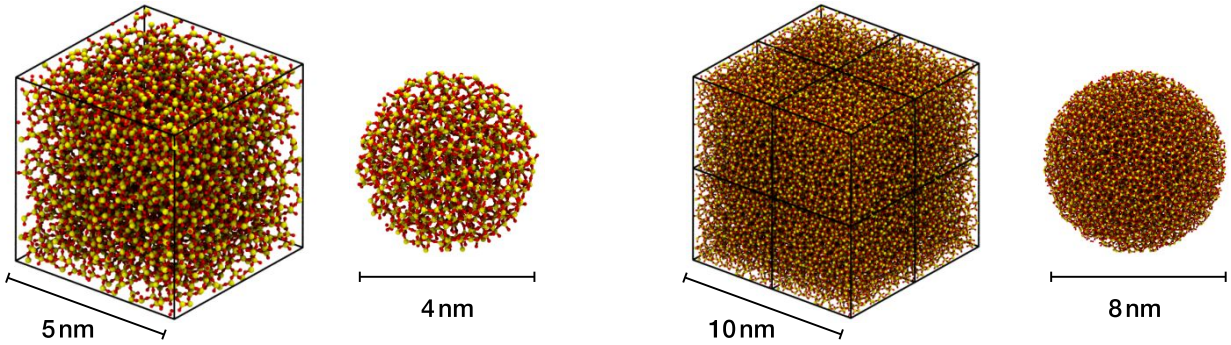


**Figure S3** – Diagrams of the nanoparticles and the corresponding silica bulk used to carve them for nanoparticles with diameters of 4 and 8nm. For nanoparticles with a diameter larger than 5nm, the silica bulk is replicated.

Nanoparticles are carved from the bulk silica as spheres of a user-defined radius (i.e. all atoms within *R*(nm) from the center of the box are included in the nanoparticle). As the dimensions of the silica box are 5nm x 5nm x 5nm, nanoparticles with radii larger than 2.5nm necessitate replication of the box for carving (Fig. S3b).

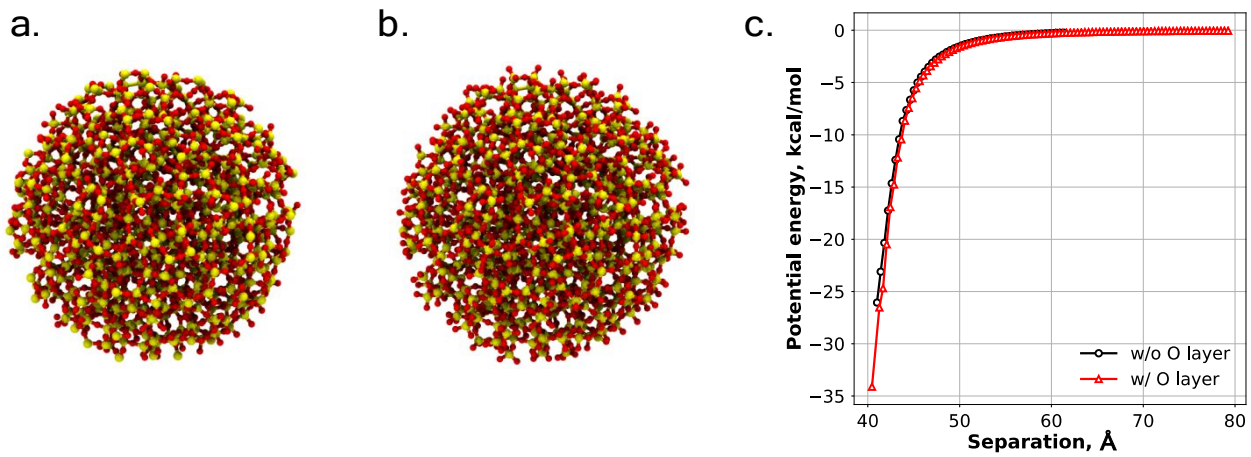


**Figure S4** – Silica nanoparticles with a diameter of 4nm a. without and b. with a surface oxygen layer. c. The interaction energy between two nanoparticles without (black) and with (red) a surface oxygen layer.

Nanoparticles carved directly from bulk as perfect spheres certainly represent an idealized model, where in reality one would expect silica nanoparticles to feature some asphericity and a hydroxylized outer layer. The influence of an outer oxygen layer is examined by calculating the interaction potential between two nanoparticles, comparing the model described in the main text (Fig. S4a, where nanoparticles are carved "as is" without an outer oxygen layer) with a model where an additional buffer of oxygen atoms (0.275nm) is included (Fig. S4b). For the model that includes oxygen atoms, Si-O bonds were generated between all atoms within 0.20419nm and any atoms that are left un-bonded are removed from the system. The interaction potential calculated using these two models is shown in Fig. S4c, where it should be noted that we have shifted the curve for the second model (w/ oxygen atoms) by a value of -0.55nm (twice the oxygen buffer) to account for the difference in radii. From Fig. S4c we observe that the presence of an oxygen layer does not appreciably influence the nanoparticle-nanoparticle interaction potential. This helps provide further justification for the use of the simpler, idealized model we have utilized for the target data in the main text.

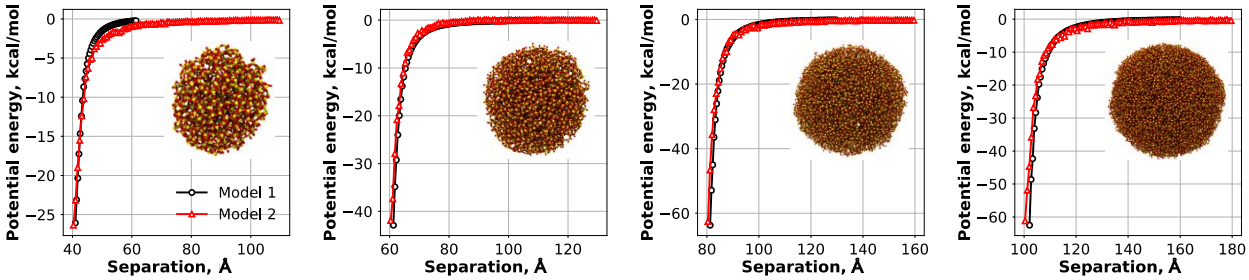


**Figure S5** – The interaction energy between nanoparticles with diameters of 4, 6, 8, and 10nm using two different model. In black is the model used in the main text, where nanoparticles are carved directly from bulk silica. In red are nanoparticles that are equilibrated after carving.

Concerning asphericity, in earlier trials of our nanoparticle optimizations we utilized target data obtained from nanoparticles that had been equilibrated for 50ps using the ReaxFF force field. For small nanoparticles (e.g. $R$=2nm) considerable asphericity was observed which resulted in difficulty obtained coarse-grained parameters that fit to the all-atom target data, as the coarse-grained nanoparticles are constructed as perfect spheres. Fig. S5 shows the interaction potential between two nanoparticles, comparing results obtained using two nanoparticle models:

- **Model 1**: The model described in the main text, where nanoparticles are carved directly from bulk silica as (nearly) perfect spheres with no additional adjustments.
- **Model 2**: After carving from bulk silica, nanoparticles are equilibrated for 50ps under the ReaxFF force field. The interaction potential between two nanoparticles is calculated using DREIDING force field and includes a Coulomb term that uses charges from the ReaxFF charge equilibration.

It can be observed that for nanoparticles with radii of 3, 4, and 5nm the interaction potential is nearly identical between the two models. For the smallest nanoparticle size ($R$=2.5nm) deviation between the two models is observed, likely due to the asphericity of the nanoparticle in Model 2 (pictured as an inset). The agreement observed between these two models further supports the

use of the idealized model (Model 1) for target data collection in the main text, and suggests that asphericity effects are negligible for radii ≥ 3nm.

**Atomistic force field**

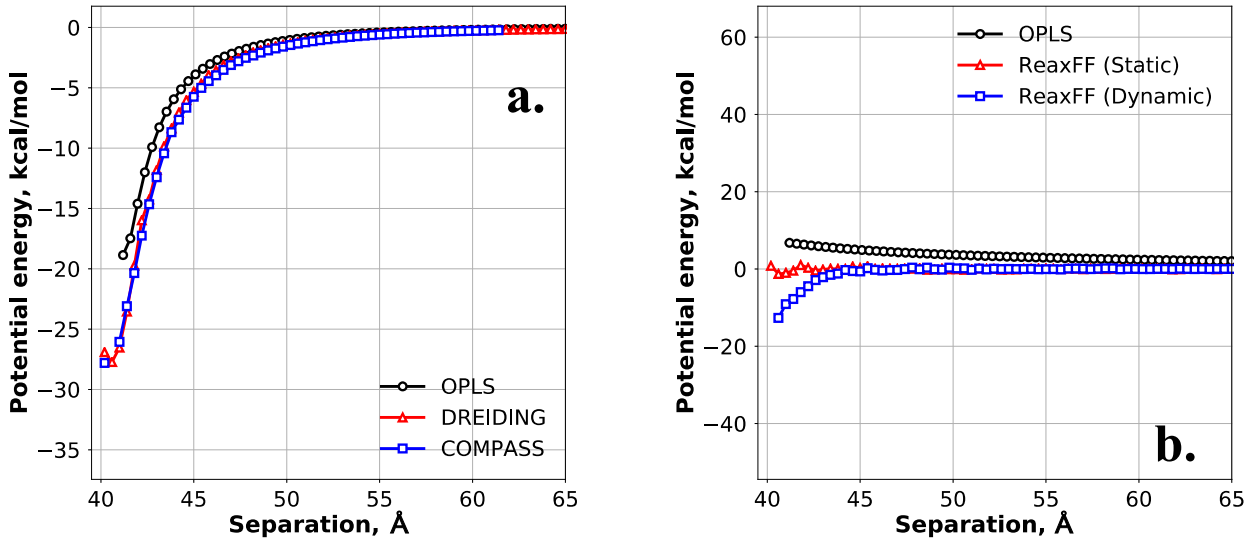


**Figure S6** – a. The interaction energy *considering VDW interactions only* between two nanoparticles with d=4nm using the OPLS (black circles), DREIDING (red triangles), and COMPASS (blue squares) force fields. b. The interaction energy *considering electrostatic interactions only* using OPLS charges (black circles), charges obtained from ReaxFF charge equilibration (red triangles), and ReaxFF charges updated at each timestep (blue squares).

Nanoparticle-nanoparticle interaction potential *considering VDW interactions only* is examined using LJ parameters from three force fields: hybrid COMPASS, DREIDING, and OPLS. The hybrid COMPASS force field uses a 9-6 Class2 Lennard-Jones-like potential (Eq. 2 in the main text) and the following sixth-order mixing rules for cross interactions:

$$\sigma_{Si-O} = \left(\frac{\sigma_{Si}^6 + \sigma_O^6}{2}\right)^{\frac{1}{6}} \quad \text{(S1)}$$

$$\varepsilon_{Si-O} = \left(\frac{2\sigma_{Si}^3\sigma_O^3\sqrt{\varepsilon_{Si}\varepsilon_O}}{\sigma_{Si}^6 + \sigma_O^6}\right) \quad \text{(S2)}$$

Additional details on the hybrid COMPASS LJ parameters are located in the main text.[6,7] Both the OPLS and DREIDING force fields describe VDW interactions through a 12-6 LJ potential,

using Lorentz-Berthelot mixing rules for cross interactions. OPLS LJ parameters for silicon are $\sigma_{Si}$ =4.0Å and ε=0.10kcal/mol, and for oxygen are $\sigma_O$=3.0Å and ε=0.17kcal/mol.[8] DREIDING LJ parameters for silicon are σ=3.804Å and ε=0.310kcal/mol, and for oxygen are σ=3.033Å and ε=0.096kcal/mol.[9] The VDW contribution to the interaction potential is shown in Fig. S6 for nanoparticles with a diameter of 4nm. Interaction potentials calculated using the DREIDING and COMPASS force fields are shown to be nearly identical, whereas the OPLS curve is shown to be slightly smoother. As both the DREIDING and COMPASS force fields have been utilized in the literature in studies of silica nanoparticles, it was determined that one of these should be chosen for our study. Interactions potentials were calculated slightly quicker using the COMPASS force field, so this is the one that was ultimately chosen.

Nanoparticle-nanoparticle interaction potential *considering electrostatic interactions only* is examined using three sets of partial charges: OPLS, partial charges obtained through ReaxFF charge equilibration (QEq-static), and partial charges obtained through ReaxFF charge equilibration that are updated at each configuration (QEq-dynamic). OPLS charges for silicon and oxygen are 0.86 and -0.43 respectively.[8] Charge equilibration was performed in LAMMPS using the implementation by Aktulga et al..[10] The electrostatic contribution to the interaction potential is shown in Fig. S6b for nanoparticles with a diameter of 4nm. The electrostatic contribution to the interaction potential using OPLS charges is shown to yield large error bars and deviates to slightly positive values at smaller separations. This is expected, as fixed charges without a charge equilibration are likely to yield a non-uniform charge distribution, and the lack of considering nanoparticle charge neutrality during carving is likely to provide each nanoparticle with a slight charge that will lead to repulsion. The electrostatic contribution to the

interaction potential using dynamic charge equilibration is shown to be negligible at long range, and reveals attraction at short range. However, as mentioned in the main text, silica nanoparticles typically feature a polymer coating to prevent aggregation, so we are not concerned with the short range behavior, thus, the influence of charge appears to be negligible as has been found in previous work comparing the influence of various force fields on silica nanoparticle self-assembly.[11] This is further supported by examining the electrostatic contribution to the interaction potential using charges obtained through a single charge equilibration. Here, the influence of charge is shown to be negligible even at short range.

**Target data collection (nanoparticle-nanoparticle)**

Target data used in force field optimization consists of values of interaction potential between two bodies calculated over a range of center-of-mass separations. For optimization of nanoparticle-nanoparticle parameters, the two bodies involved in target data collection are atomistic nanoparticles. Target data collection is not included within the Python package we have developed, as we opted for scripting in C++ for this portion of the development for ease of parallelization and improved performance. A template of the script used in the collection of target data is provided in the GitHub repository.[4] The procedure used to collect target data can be broken down as:

1. Load in the atomic positions from an XYZ file
2. Define limits of center-of-mass separations to examine
   - **Min**: $d$
   - **Max**: $d + 4 + \text{ceil}(d/4) - 1$
   - This does not represent the range of the final data, as pruning is performed to remove values at short separations (within the region of overlapping VDW volumes), described in further detail below.
3. Initialize a histogram with 100 bins (higher resolution is therefore provided to smaller nanoparticles)
4. Choose a starting separation within the range of (Min, Max)
5. Evaluate the interaction energy and add the value to the appropriate bin in the histogram
   - Note: An overlap criterion is considered whereby if any two atoms are of a distance $\leq 0.8\sigma$ the two nanoparticles are considered to be overlapping and this configuration is skipped. This helps to avoid contributions from high-energy, overlapping configurations at small center-of-mass separations that systems would be unlikely to adopt.
6. Generate a new configuration by randomly rotating and randomly translating one of the nanoparticles

7. Continue to repeat steps 5 and 6 until an even sampling of all bins is achieved (excluding the first 5 bins, where our overlap criterion inhibits even sampling)

After target data is collected, the data is pruned to remove values at center-of-mass separations below 0.40323nm x 0.8, again as an overlap criterion, where 0.40323nm represents the diameter of silica. This removes data at center-of-mass separations where VDW radii would be overlapping, which hinders optimization of coarse-grained parameters.

It should also be noted that the number of configurations sampled per bin is not equal for all nanoparticle radii; however, standard deviations in interaction potential for all radii and center-of-mass separations are <10% and are closer to <2% for values other than at the shortest few center-of-mass separations. This supports the notion that a sufficient number of configurations were sampled per bin for all nanoparticle sizes. As follows are the mean number of configurations per bin, along with the standard deviation, for each of the radii examined in this work (3nm-10nm) is as follows: 3nm: 86.8 ± 9.2, 4nm: 69.5 ± 10.1, 5nm: 22.4 ± 4.2, 6nm: 66.1 ± 9.7, 7nm: 33.6 ± 5.2, 8nm: 19.1 ± 3.5, 9nm: 25.6 ± 4.2, 10nm: 13.9 ± 3.8.

**Target data collection (nanoparticle-alkane cross-interactions)**

Target data was also collected for the interaction between spherical silica nanoparticles of various radii and united-atom alkane moieties ($CH_2$, $CH_3$). Data collection used the same procedure as for the target data collected for the potential between two nanoparticles, evaluating the interaction energy at a series of center-of-mass separations. It was determined that additional data needed to be collected in the region of the potential well, and further determined that additional long-range data was required. As such, target data collection used the following general procedure three separate times, with values for the minimum and maximum center-of-mass separations and bin numbers in parentheses corresponding to the three separate iterations:

1. Load in the atomic positions from an XYZ file
2. Define a single point to represent the united-atom CH2 or CH3 moiety
3. Define limits of center-of-mass separations to examine
    - **Min**: ($d$/2, $d$/2 + 0.2, $d$/2 + 1.0)
    - **Max**: ($d$/2 + 1.0, $d$/2 + 0.4, $d$/2 + 3.0)
    - This does not represent the range of the final data, as pruning is performed to remove data with large error bars in the short-range region and additional data was collected to provide additional fidelity to the region of the potential well. See further explanation below.
4. Initialize a histogram with (50, 50, 20) bins
5. Choose a starting separation within the range of (Min, Max)
6. Evaluate the interaction energy and add the value to the appropriate bin in the histogram
    - Note: An overlap criterion is considered whereby if any two atoms are of a distance $\leq 0.8\sigma$ the two nanoparticles are considered to be overlapping and this configuration is skipped. This helps to avoid contributions from high-energy, overlapping configurations at small center-of-mass separations that systems would be unlikely to adopt.

7. Generate a new configuration by randomly rotating and randomly translating the nanoparticle
8. Continue to repeat steps 5 and 6 until an even sampling of all bins is achieved

The three iterations produced three sets of data, and a complete set was generated by combining these three and running a function that ensured the data monotonically decreased to the bottom of the potential well and monotonically increased after. Points that did not satisfy this criterion were deleted. This was necessary as the standard deviation in the short-range region was quite high, yet a defined well was found necessary for successful optimization.

**Equations used from the work of Lee and Hua for CG model comparison**

To compare the CG model developed in this work with available models in the literature, Fig. 11 in the main text provides plots showing interaction potential curves for several nanoparticle sizes calculated using the model developed in this work and using equations provided in Fig. 6 of the work by Lee and Hua.[12] In their work, a general interaction potential was used for the interaction between two point nanoparticles of the form:

$$U(r) = 4\varepsilon\left[(\sigma/r)^{2\alpha} - (\sigma/r)^{\alpha}\right]$$

where $\sigma$ is the nanoparticle diameter and $\varepsilon$ and $\alpha$ are derived through fitting. The equations derived via fitting (along with reduced forms of $\varepsilon$ and $\sigma$) for these last two parameters are:

$$\varepsilon_r = {}^{\varepsilon}\!/_{\varepsilon_0}$$

$$\sigma_r = {}^{\sigma}\!/_{\sigma_0}$$

$$\varepsilon_r = 286[1 - \exp(-0.014\sigma_r)]$$

$$\alpha = 0.226 + 2.983\sigma_r$$

where $\sigma_0$ and $\varepsilon_0$ correspond to 0.62nm and 3.10 kJ/mol, respectively. The values for $\sigma_0$ and $\varepsilon_0$ correspond to the parameters used in the interaction between pseudo-atoms of a coarse-grained nanoparticle model similar to that used in our work; however, in the work of Lee and Hua, pseudo-atoms were fixed to a given size (0.62nm in diameter) and interactions were governed by a 12-6 Lennard-Jones potential. The equations above for point particle interactions have been used in our main text (Figure 11) to compare nanoparticle-nanoparticle interaction potential curves with our model.

**States considered for parameterization of nanoparticle-nanoparticle core interactions**

Parameterization of nanoparticle-nanoparticle core interactions followed the procedure outlined in Fig. 2 of the main text. Specifically, Stages 1 and 2 of the optimization scheme were performed for all nanoparticles described by:

- $d$(nm): 4, 6, 8, 10, 12, 14, 16, 18, 20
- $\sigma_b$(nm): 0.5, 0.6, 0.7, 0.8, 0.9, 1.0, 1.1, 1.2, 1.3, 1.4, 1.5, 1.6, 1.7, 1.8, 1.9, 2.0
- $\varphi_b$: 0.25, 0.30, 0.35, 0.40, 0.45, 0.50, 0.55, 0.60

It should be noted that the following two exclusion criteria were applied to remove a small subset of state points:

- Nanoparticles where $d/\sigma_b > 20$, as these systems are finely-grained and add significant computational expense to the optimization
- States featuring regions of intersection between three neighboring pseudo-atoms, as the volume of this intersection region cannot be easily calculated, and thus these systems cannot be constructed with a reliable $\varphi_b$. These systems typically feature $d \leq 6$nm and $\sigma_b \geq 1.3$nm.

Following these two exclusion criteria, 1010 states remained for the optimization.

*Corresponding Author: Clare McCabe, Email: c.mccabe@vanderbilt.edu 

**Interactions between nanoparticles with different $d$, $\sigma_b$, and $\varphi_b$**

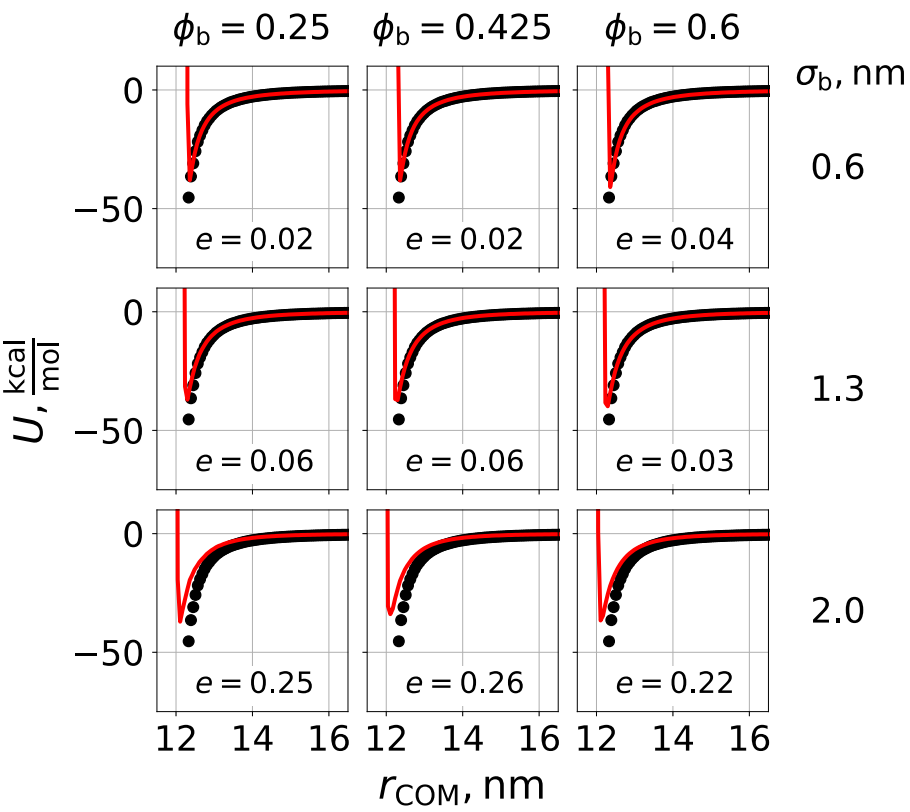


**Figure S7** – Interaction potential between a nanoparticle with $d$=8nm, $\sigma_b$=0.6nm, and $\varphi_b$=0.4 and a nanoparticle with $d$=16nm, $\sigma_b$=0.6, 1.3 and 2.0nm, and $\varphi_b$=0.25, 0.425, and 0.6. Points represent all-atom data and lines represent CG data using parameters obtained from Eqs. 6 and 7 and the mixing rules detailed in the main text.

Fig. S7 shows an expanded version of Fig. 7a-c from the main text, comparing the derived CG potential against all-atom data for nanoparticles of different sizes. As noted in the main text, it is observed that increasing $\sigma_b$ of the larger nanoparticle results in higher residual values; however, the curves in general show excellent fits considering the simplicity of the mixing rules used. Fig. S7 also shows that the residual between the CG and all-atom data for nanoparticles of different sizes is independent of $\varphi_b$.

**References**


(1) mBuild: a component-based molecule builder tool that relies on equivalence relations for component composition. http://mosdef-hub.github.io/mbuild/ (accessed Jul 10, 2017).

(2) Klein, C.; Sallai, J.; Jones, T. J.; Iacovella, C. R.; McCabe, C.; Cummings, P. T. A Hierarchical, Component Based Approach to Screening Properties of Soft Matter. In *Foundations of Molecular Modeling and Simulation*; 2016; pp 79–92.

(3) Colbert, C. Post on Numpy discussion list http://mail.scipy.org/pipermail/numpy-discussion/2009-July/043811.html.

(4) Summers, A. Z.; Iacovella, C. R.; Cane, O. M.; Cummings, P. T.; McCabe, C. NanoOpt: Deriving potentials for coarse-grained nanoparticles via potential-matching https://github.com/mosdef-hub/nanoparticle_optimization (accessed Dec 8, 2018).

(5) Litton, D. A.; Garofalini, S. H. Modeling of Hydrophilic Wafer Bonding by Molecular Dynamics Simulations. *J. Appl. Phys.* **2001**, *89* (11), 6013–6023.

(6) Sun, H. Ab Initio Calculations and Force Field Development for Computer Simulation of Polysilanes. *Macromolecules* **1995**, *28* (3), 701–712.

(7) Sun, H.; Rigby, D. Polysiloxanes: Ab Initio Force Field and Structural, Conformational and Thermophysical Properties. *Spectrochim. Acta - Part A Mol. Biomol. Spectrosc.* **1997**, *53* (8), 1301–1323.

(8) Lorenz, C. D.; Webb, E. B.; Stevens, M. J.; Chandross, M.; Grest, G. S. Frictional Dynamics of Perfluorinated Self-Assembled Monolayers on Amorphous SiO2. *Tribol. Lett.* **2005**, *19* (2), 93–98.

(9) Mayo, S. L.; B.D.Olafson; Iii, W. a G. DREIDING: A Generic Force Field for Molecular Simulations. *J. Phys. Chem.* **1990**, *94* (Suite 540), 8897–8909.

(10) Aktulga, H. M.; Fogarty, J. C.; Pandit, S. a.; Grama, a. Y. Parallel Reactive Molecular Dynamics: Numerical Methods and Algorithmic Techniques. *Parallel Comput.* **2012**, *38* (4–5), 245–259.

(11) Ionescu, T. C.; Qi, F.; McCabe, C.; Striolo, A.; Kieffer, J.; Cummings, P. T. Evaluation of Force Fields for Molecular Simulation of Polyhedral Oligomeric Silsesquioxanes. *J. Phys. Chem. B* **2006**, *110* (6), 2502–2510.

(12) Lee, C. K.; Hua, C. C. Nanoparticle Interaction Potentials Constructed by Multiscale Computation. *J. Chem. Phys.* **2010**, *132* (22), 224904.